BIOCHEMISTRY
including biophysical chemistry & molecular biology

Article

pubs.acs.org/biochemistry

Origin of the Enigmatic Stepwise Tight-Binding Inhibition of Cyclooxygenase-1

Yasmin Shamsudin Khan, Masoud Kazemi, Hugo Gutiérrez-de-Terán, and Johan Åqvist*

Department of Cell and Molecular Biology, Uppsala University, Box 596, BMC, SE-751 24 Uppsala, Sweden

ABSTRACT: Nonsteroidal anti-inflammatory drugs (NSAIDs) are widely used for the treatment of pain, fever, inflammation, and some types of cancers. Their mechanism of action is the inhibition of isoforms 1 and 2 of the enzyme cyclooxygenase (COX-1 and COX-2, respectively). However, both nonselective and selective NSAIDs may have side effects that include gastric intestinal bleeding, peptic ulcer formation, kidney problems, and occurrences of myocardial infarction. The search for selective high-affinity COX inhibitors resulted in a number of compounds characterized by a slow, tight-binding inhibition that occurs in a two-step manner. It has been suggested that the final, only very slowly reversible, tight-binding event is the result of conformational changes in the enzyme. However, the nature of these conformational changes has remained elusive. Here we explore the structural determinants of the tight-binding phenomenon in COX-1 with molecular dynamics and free energy simulations. The calculations reveal how different classes of inhibitors affect the equilibrium between two conformational substates of the enzyme in distinctly different ways. The class of tight-binding inhibitors is found to exclusively stabilize an otherwise unfavorable enzyme conformation and bind significantly stronger to this state than to that normally observed in crystal structures. By also computing free energies of binding to the two enzyme conformations for 16 different NSAIDs, we identify an induced-fit mechanism and the key structural features associated with high-affinity tight binding. These results may facilitate the rational development of new COX inhibitors with improved selectivity profiles.

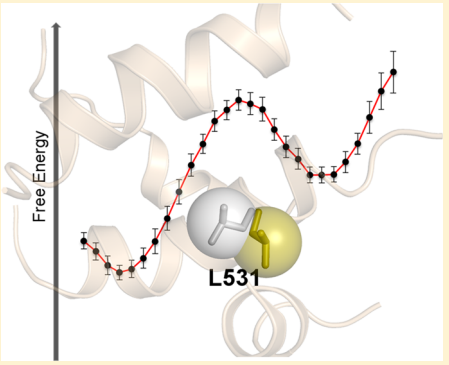

Nonsteroidal anti-inflammatory drugs (NSAIDs) make up one of the most used classes of medication. By inhibiting the enzyme cyclooxygenase (COX), they prevent the formation of various prostaglandins responsible for the physiological responses of fever, pain sensitization, and inflammation. NSAIDs inhibit the two isoforms, COX-1 and COX-2, with varying affinities and selectivities. Classical NSAIDs are competitive inhibitors and generally nonselective or preferential toward COX-1. These drugs have side effects that include gastric intestinal bleeding, peptic ulcer formation, and kidney problems.[1−3] These side effects are not present in a newer class of selective COX-2 inhibitors, commonly termed coxibs, which have been introduced to the market. However, increased occurrences of myocardial infarction leading to cardiac failure have been related to these inhibitors.[4−6] Although the most common uses of COX inhibitors are reduction of pain, fever, and inflammation, COX is also an anticancer target. COX-2 is overexpressed in epithelium-derived cancers, such as colorectal cancer,[1,7] and selective inhibition of COX-2 is a successful method for restricting cancer growth.[2,3,8] COX-1 promotes production of angiogenic growth factors and is overexpressed in ovarian cancer.[4−6,8] Similar to the use of COX-2 selective inhibitors in epithelium-derived cancers, selective inhibition of COX-1 may be a possible approach to adjuvant therapy for ovarian cancer.

The structural reasons for preferential COX-1 inhibition in classical NSAIDSs are unknown. However, it is known that inhibitors with a preference for an isoform are generally also slow-releasing high-affinity binders, or so-called "tight binders", of that isoform. The tight-binding event is time-dependent and occurs in two or three steps.[9−11] The inhibitor binds rapidly, reversibly, and with low affinity in the initial step(s) followed by time-dependent, high-affinity inhibition in the final step.[10,12−20] Although the mechanism of binding is noncovalent,[14,21,22] the final step is only very slowly reversible and in practice resembles irreversible inhibition.

The time-dependent tight-binding event has been hypothesized to result from conformational changes in the enzyme.[10,12−20,22,23] Understanding the molecular mechanisms of tight binding could be key to understanding selectivity, thus allowing the design of drugs with tuned selectivity for different isoforms. Although the conformational changes are unknown, the resulting high-affinity binding can be probed under certain assay conditions. Assays are thus constructed so that the enzyme is preincubated with the inhibitor while the substrate is added to the mixture at fixed time intervals and the inhibition of the catalytic process is monitored over time.[10,14,22,24,25] Time-dependent inhibitors typically bind in the micromolar range at very short incubation times, and in instant inhibition assays where the reaction is started by adding enzyme to a mixture of substrate and inhibitor. However, as the preincubation time increases, the affinities of these compounds

Received: September 16, 2015
Revised: November 5, 2015
Published: November 12, 2015

DOI: 10.1021/acs.biochem.5b01024
Biochemistry 2015, 54, 7283−7291

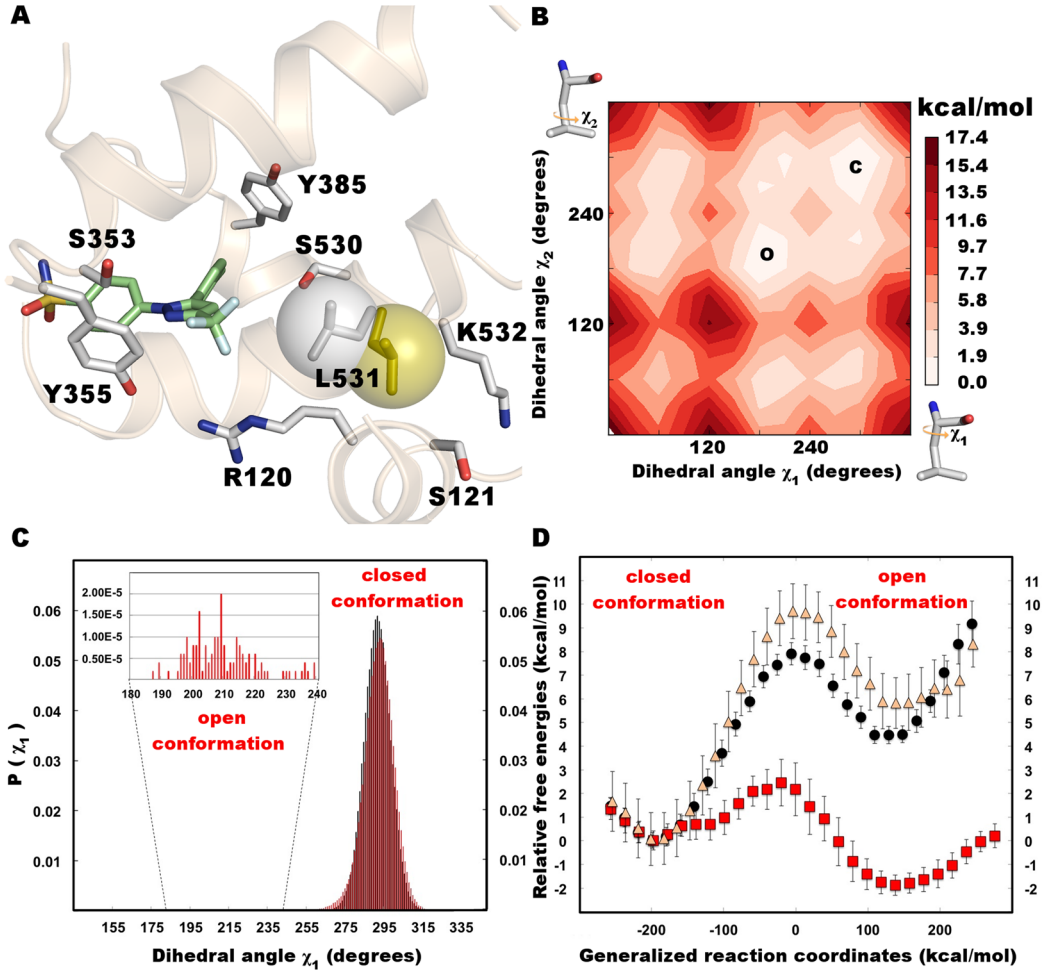

Figure 1. (A) Closed (gray) and open (gold) conformations of hCOX-1 modeled according to the crystal structures of oCOX-1 (PDB entries 1Q4G and 4O1Z, respectively).[29,31] The COX-2 selective inhibitor celecoxib is overlaid from the crystal structure for reference. (B) Map of the two-dimensional rigid coordinate scans, where the closed (C) and open (O) conformations are marked. (C) Histogram of the probability density of χ_1 dihedral angles from unbiased MD simulations of apo hCOX-1. The black area represents simulations starting from the closed conformation and the red area simulations starting from the open conformation. (D) Average free energy profiles from PMF calculations of apo hCOX-1 (black circles) and hCOX-1 in complex with the slow, tight-binding inhibitor flurbiprofen (red squares) and the reversible, competitive inhibitor ibuprofen (orange triangles). Note that the error bars reported are standard deviations because the standard errors of the mean were too small to visualize in the plot.

can increase into the nanomolar range. This is the case both for irreversible inhibitors, such as the time-dependent inhibitor Aspirin (which irreversibly acetylates Ser530 of the COX enzymes), and for the slowly reversible (tight-binding) inhibitors, herein termed Class I inhibitors. Examples of Class I inhibitors considered in this study are the COX-1 selective inhibitors indomethacin and flurbiprofen, which are competitive inhibitors with typical slow tight-binding kinetic profiles.[26] In contrast to time-dependent inhibitors, time-independent Class II compounds such as the nonselective, competitive, and reversible NSAID ibuprofen display no significant difference in affinities between the two assay types. However, there are also examples of molecules belonging to a mixed-type class, Class III, which are neither competitive, reversible nor classic time-dependent inhibitors but instead are classified as slow reversible inhibitors.[27] The COX-2 selective compound meloxicam[28] is an example of the inhibitors that belong to this category.

Recent crystal structures of oxicam complexes with ovine and murine COX-1 and COX-2 surprisingly revealed a novel binding mode not seen before for NSAID complexes[29] and also showed that the enzyme conformation can vary depending on the ligand bound. Moreover, the size of the binding pocket was found to be modulated mainly by the orientation of a single side chain (Leu531).[29−31] Here, we explore the hypothesis that the existence of these conformational substates may be related to the tight-binding phenomenon, using molecular dynamics (MD) free energy calculations to characterize the binding energetics of different classes of inhibitors in human COX-1. Besides confirming the existence of two stable enzyme conformations (Figure 1A), the computer simulations reveal a distinct correlation between the conformation of Leu531 and high-affinity binding for slow, tight-binding inhibitors. Hence, a significantly higher affinity is predicted for these compounds in the open conformation, but not for other classes of inhibitors. We further show that tight-binding inhibitors stabilize the open conformation relative to the otherwise favored closed one. Conversely, time-independent, competitive reversible inhibitors are predicted to destabilize the open conformation and increase the activation barrier for transition between the two states. These results thus rationalize the elusive tight-binding phenomenon and open up new possibilities of tuning the selectivity of drugs acting on the COX enzymes.

DOI: 10.1021/acs.biochem.5b01024
Biochemistry 2015, 54, 7283−7291

METHODS

Molecular Dynamics (MD) Simulations. Human COX-1 (hCOX-1) structures were constructed by homology modeling using a closed conformation ovine COX-1 (oCOX-1) structure (PDB entry 1Q4G)[31] as the template. It was set up for MD simulations as described previously,[9] except for the rotation of Leu531, modeled according to an open conformation oCOX-1 structure (PDB entry 4O1Z).[29] All simulations were performed using the molecular dynamics program Q[32] with the OPLS-AA force field[33] and solvated with TIP3P[34] water molecules. Spherical boundary conditions were used, with a sphere with a radius of 20 Å centered on the C12 atom of the ligand cocrystallized in the template 1Q4G. The sequence identity is 94% within the simulation sphere, and the orientations of side chains within the binding pocket were preserved by homology modeling. The water boundary of the system was subject to polarization and radial constraints according to the surface-constrained all-atom solvent (SCAAS) model[32,35] at the sphere surface to mimic the properties of bulk water. Nonbonded interactions were calculated explicitly up to a 10 Å cutoff, except for the ligand atoms for which no cutoff was used. Beyond the cutoff, long-range electrostatics were treated with the local reaction field multipole expansion method.[36] Water bonds and angles, as well as solute bonds, were constrained with the SHAKE[37] algorithm. Nonbonded pair lists were updated every 25 steps, and the same interval was used for the sampling of the ligand-surrounding interaction energies.

Protein atoms outside the simulation sphere were restrained to their initial positions and interacted with the system through only bonds, angles, and torsions. The ionization states of titratable residues inside the simulation sphere were manually assessed with the following residues treated as ionized: Asp190, Glu520, Glu524, Arg120, His90, and His513. Ionizable residues close to the sphere boundary were modeled in their neutral form to account for dielectric screening. With this setup, the simulation sphere was overall neutral, except for the charge of ligands bearing a carboxylate group. Hence, the protein and water (reference) simulation systems have the same net charge and thus avoid the consideration of additional Born terms in the calculation of free energies. The system was slowly heated with positional restraints on all solute heavy atoms gradually released as the temperature was increased to its target value for data collection (298 K). The MD time step was also gradually increased from 0.2 to 2 fs. During the subsequent 2 ns equilibration phase, no restraints were applied. The potential of mean force (PMF) calculations were conducted with a 1 fs time step and no solute bond constraints.

As noted earlier, the computational strategy using truncated spherical simulation systems has proven to be very efficient for doing many independent free energy calculations, which is necessary for attaining reliable statistics.[38] The goal in this case is thus not to simulate the dynamics of conformational fluctuations distal to the binding site (which usually have negligible effects on ligand binding energetics far away) but to obtain free energy estimates that are as reliable as possible, at a computational cost that allows many ligands to be evaluated. In this respect, reduced models that have been shown to yield correct local structural fluctuations[39] of the binding site may be significantly more efficient than larger scale models, precisely because they do not sample large scale conformational motions that require much longer time scales for convergence. Note, however, that long-range electrostatic interactions may still yield non-negligible contributions to the binding energetics of, in particular, charged compounds.[40] The energetics of such interactions can be treated in a mean field manner (similar to Poisson−Boltzmann calculations) without requiring extensive conformational sampling far from the binding site (see below).

Conformational Analysis. A conformational scan was done using the two-dimensional coordinate scan tool of Schrödinger's MacroModel software[41] to roughly assess the energy landscape. The χ_1 (C_γ−C_β−C_α−N) and χ_2 (C_δ−C_γ−C_β−C_α) dihedral angles (Figure 1B) of Leu531 were rotated in 12° increments in apo hCOX-1 using a continuum solvent and the OPLS2005 force field,[33] and the energies were plotted against the angles. The scan was followed by 10 replicates of unbiased MD simulations, each 50 ns in duration (totaling 0.5 μs) following an additional equilibration phase of 10 ns, using the OPLS-AA force field,[33] the TIP3P water model,[34] and the molecular dynamics package Q.[32] Five simulations started from the open state and five simulations from the closed state to assess the occupancy of various conformations unbiased with respect to starting conformation. The conformation was sampled every 0.5 ps and the corresponding χ_1 torsion value extracted. The reported plot was constructed as a probability distribution over histogram bins of χ_1 dihedral angles (Figure 1C).

Potential of Mean Force Calculations. PMF calculations were performed using the C_γ−C_β−C_α−N dihedral angle (χ_1) of Leu531 as a variable, starting from the open conformation of the solvated apo structure. Following an additional 10 ps equilibration phase in which the MD step size was reset to 1 fs, the dihedral angle was pushed from 0° to 180° in 800 discrete windows, each 30 ps in duration, following the procedure of Wallin et al.[42] Here, the transformation from the open to the closed state utilizes the biased force field potentials

$$U^{\mathrm{O}} = U^{\mathrm{FF}} - U^{\mathrm{FF}}_{\mathrm{tor}}(\chi) + U^{\mathrm{O}}_{\mathrm{b}}(\chi)$$

$$U^{\mathrm{C}} = U^{\mathrm{FF}} - U^{\mathrm{FF}}_{\mathrm{tor}}(\chi) + U^{\mathrm{C}}_{\mathrm{b}}(\chi) \quad (1)$$

for the open and closed states, respectively. $U^{\mathrm{FF}}_{\mathrm{tor}}(\chi)$ is the torsion term for χ_1 in the regular force field potential (U^{FF}), and $U^{\mathrm{O}}_{\mathrm{b}}$ and $U^{\mathrm{C}}_{\mathrm{b}}$ are biasing potentials for the open and closed states, respectively. These are quadratic, $U_{\mathrm{b}} = k(\chi - \chi_0)^2$, with a 75 kcal mol^{-1} rad^{-2} force constant (k), and their respective minima (χ_0) coincide with the open and closed conformations. The transformation is then performed via the mapping potential $U_{\mathrm{m}} = (1 - \lambda_{\mathrm{m}})U^{\mathrm{O}} + \lambda_{\mathrm{m}}U^{\mathrm{C}}$, where the mapping parameter λ_{m} is varied between 0 and 1 in 800 discrete simulation windows. The free energy change on the true force field potential surface is then obtained by removing the bias according to the umbrella sampling formula

$$\Delta G(X_n) = \sum_{m \subset X_n} w_m \{\Delta G(\lambda_m) - RT \ln \langle e^{-[U^{\mathrm{FF}}(X_n) - U_m(X_n)]/RT} \rangle_m \} / \sum_{m \subset X_n} w_m \quad (2)$$

where X_n is our discretized reaction coordinate, defined as $X_n = U^{\mathrm{O}} - U^{\mathrm{C}}$, and the relevant energy values (U^{FF} and U_m) are binned with respect to X_n. The first term on the right-hand side of eq 2 is the free energy associated with moving on the mapping potential and is computed as the average of forward and reverse application of the free energy perturbation equation

DOI: 10.1021/acs.biochem.5b01024
Biochemistry 2015, 54, 7283−7291

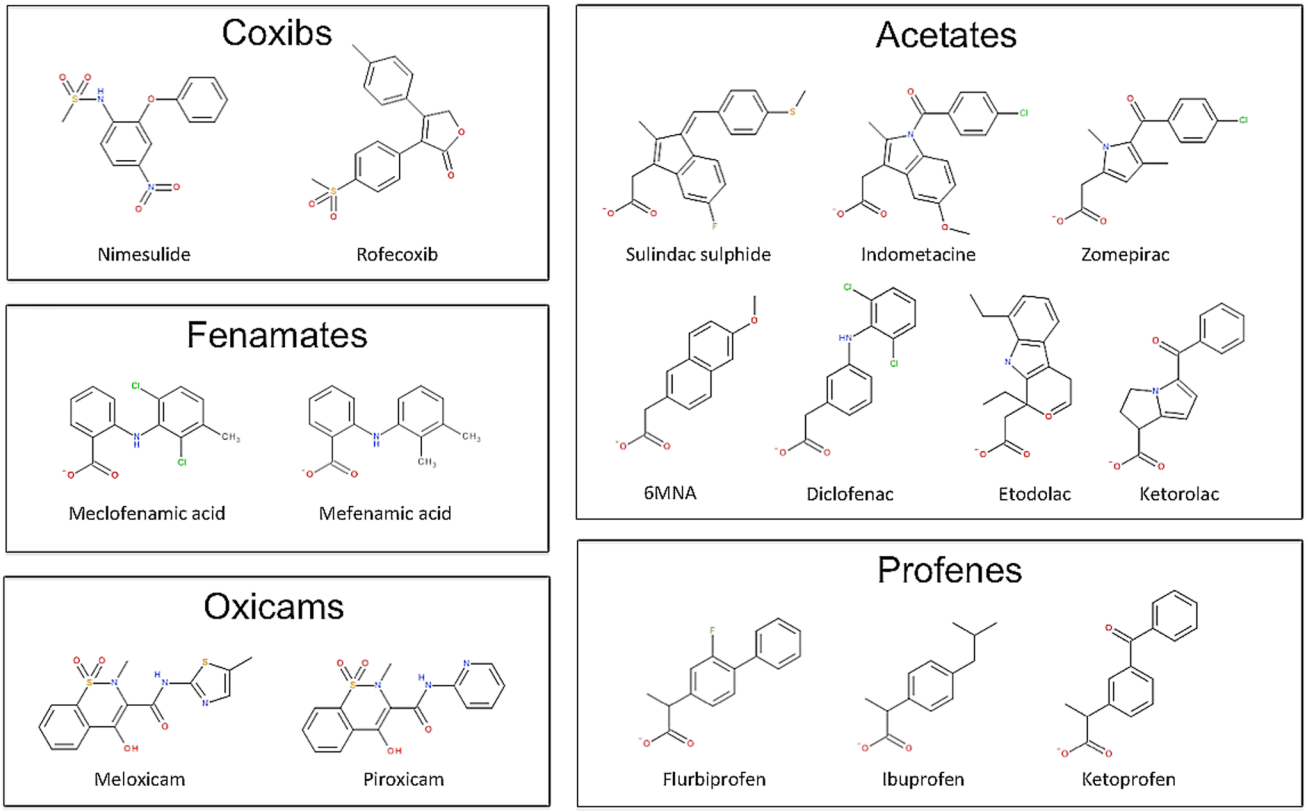

Figure 2. Chemical structures of the compounds studied herein divided according to structural class, except for nimesulide and celecoxib, which are grouped on the basis of their selectivity for COX-2.

Table 1. Calculated and Experimental Binding Free Energies for hCOX-1[a]

ligand	$\Delta G_{bind}^{calc(open)}$	$\Delta G_{bind}^{exp(incubated)}$[b]	$\Delta G_{bind}^{exp(instant)}$[c]	$\Delta G_{bind}^{calc(closed)}$[d]
		Class I: Slow, Tight-Binding Inhibitors		
diclofenac	−8.6 ± 0.2	−10.3 ± 0.4	−7.6 ± 0.2	−7.7 ± 0.9
flurbiprofen	−10.6 ± 1.2	−10.8 ± 0.8	−8.6 ± 0.1	−9.1 ± 0.7[e]
indometacine	−10.4 ± 0.3	−10.0 ± 0.3	−6.6 ± 0.1	−6.7 ± 0.5
ketoprofen	−10.0 ± 1.3	−10.8 ± 0.4	[g]	−8.2 ± 0.6
ketorolac	−8.3 ± 0.5	−10.0 ± 0.7	−6.1 ± 0.2	−4.7 ± 0.2
meclofenamic acid	−9.6 ± 0.4	−10.3 ± 0.8	−7.9 ± 0.2	−7.9 ± 0.4
sulindac sulfide	−9.9 ± 1.5	−9.5 ± 0.8	−8.0 ± 0.3	−7.5 ± 0.7
zomepirac	−9.0 ± 0.6	−8.5 ± 1.1	[g]	−4.7 ± 1.5
		Class II: Reversible Inhibitors		
ibuprofen	−7.9 ± 1.0[f]	−7.9 ± 0.4	−7.4 ± 0.1	−6.4 ± 0.9
nimesulide	−7.8 ± 1.3[f]	−7.7 ± 0.4	[g]	−6.5 ± 0.9
rofecoxib	−5.8 ± 0.1[f]	−5.6 ± 0.1	[g]	−5.7 ± 0.3
		Class III: Slow, Reversible Inhibitors		
6MNA	−6.3 ± 0.6	−6.3 ± 0.5	−5.7 ± 0.1	−6.7 ± 0.2
etodolac	−6.6 ± 1.1	−6.9 ± 0.4	−5.6 ± 0.1	−5.7 ± 0.6
mefenamic acid	−7.5 ± 0.3	−8.1 ± 1.2	[g]	−7.4 ± 0.9
meloxicam	−8.5 ± 0.4	−7.7 ± 0.5	[g]	−8.0 ± 0.5
piroxicam	−7.3 ± 0.8	−7.5 ± 0.5	−6.5 ± 0.1	−7.3 ± 0.4

[a]All energies are in kilocalories per mole, with error bars of ±1 sem for calculated values. [b]Average binding free energies from preincubated assays ±1 sem.[12,13,15−20] [c]Binding free energies from experimental instant inhibition assays ±1 standard deviation.[21] [d]Values taken from our previous study.[9] [e]Both closed and open states were sampled in the simulations. [f]Spontaneously converged to the closed conformation. [g]Not experimentally determined.

$$\Delta G(\lambda_m) = -RT \sum_{n=0}^{m-1} \ln\langle e^{-(U_{n+1}-U_n)/RT}\rangle_n \quad (3)$$

Because a given value of the reaction coordinate X_n is sampled by multiple windows, their contribution is weighted in eq 2 with the number of data points from each λ_m by the factor $w_m/\sum w_m$. The PMF simulations were repeated five times for each system, and the reported free energy profile is the average over these five replicates. To judge convergence, standard errors of the mean (sem) were calculated over all pooled data points in

DOI: 10.1021/acs.biochem.5b01024
Biochemistry 2015, 54, 7283−7291

each bin, and the maximal sem was 0.56 kcal mol^{-1}. The average hysteresis error obtained from forward and reverse application of eq 3 for the entire transformation is <0.02 kcal/mol.

Binding Free Energy Calculations. Sixteen COX-1 inhibitors (Figure 2) that belong to different kinetic and structural classes (Table 1) were docked into a homology model of human COX-1. Each ligand was docked in 5−10 poses to probe the binding free energies. Ligands were manually placed according to the docking pose reported in our previous study[9] and in poses where the ligand occupies the novel shallow pocket formed by the rotation of Leu531 in the open conformation (Figure 1A). Note that this procedure is necessary because automated docking in this case is not reliable.[9] Binding free energies were calculated using the linear interaction energy (LIE) method[9,43,44]

$$\Delta G_{\mathrm{bind}}^{\mathrm{calc}} = \alpha\Delta\langle U_{\mathrm{l-s}}^{\mathrm{vdw}}\rangle + \beta\Delta\langle U_{\mathrm{l-s}}^{\mathrm{el}}\rangle + \gamma \quad (4)$$

where α and β are predetermined parameters that scale the difference (Δ) of the average ligand-surrounding electrostatic $\langle U_{\mathrm{l-s}}^{\mathrm{el}}\rangle$ and nonpolar $\langle U_{\mathrm{l-s}}^{\mathrm{vdw}}\rangle$ interaction energies, as calculated from separate trajectories of 10 ns of MD simulations of the solvated protein−ligand complex and the free ligand in water. The constant α was set to the standard value of 0.18, while β depends on the properties of the inhibitor.[44,45] The β values for all compounds in this study (Table 1) have been previously assigned according to the standard LIE parametrization.[9] The value of β is 0.50 for the negatively charged carboxylated ligands, while the singly hydroxylated neutral oxicams have a value of 0.37. The remaining coxibs, being neutral and lacking hydroxyl groups, have a β value of 0.43.[9,44] The term γ is a constant offset parameter specific for the protein and was kept fixed according to our previous study (−6.4 kcal mol^{-1}) to quantitatively compare the resulting binding free energies. The electrostatic correction term[46] for interactions of charged ligands with distant neglected ionized groups that were neutralized in the simulations ($\Delta G_{\mathrm{corr}}^{\mathrm{el}}$ = −1.1 kcal mol^{-1}) was determined previously.[9]

The pose resulting in the lowest binding free energy based on the LIE method from this initial screening was selected as the final starting pose. Each final ligand−protein docking pose was then subjected to 5−10 independent MD simulations (10 ns each) using the same conditions but with different initial random velocities. The reported calculated binding free energies are reported as average energies over all replicates and the corresponding errors as the standard error of the mean. Experimental binding free energies ($\Delta G_{\mathrm{bind}}^{\mathrm{exp}}$) were calculated from IC_{50} values as

$$\Delta G_{\mathrm{bind}}^{\mathrm{exp}} = RT \ln K_{\mathrm{d}} = RT \ln \mathrm{IC}_{50} + c \quad (5)$$

where c is an assay-specific constant that depends on the substrate concentration and the enzymatic K_{M} value.[47] Experimental assays were offset against each other, and the constant c is implicitly included in the parameter γ.[9] The instant inhibition assay[21] was reported with errors as standard deviations, while the average value of the binding free energies from the preincubated assays[12,13,15−20] was reported with corresponding errors as the standard error of the mean.

RESULTS

Conformational Analysis. We confirmed the existence of two stable conformations of hCOX-1, open and closed (Figure 1A), by a rigid coordinate scan, direct MD simulations, and potential of mean force (PMF) calculations for the apo structure of hCOX-1. The two-dimensional coordinate scans indicated two energy minima over broad ranges of the Leu531 χ_1 and χ_2 dihedral angles (Figure 1B), corresponding to the two major observed conformations from MD simulations of the apoenzyme. In the closed conformation, Leu531 extends into and restricts the binding cavity. This is the most commonly observed conformation in crystal structures and completely dominates in MD simulations of the apoenzyme (Figure 1C). Conversely, in the open conformation, the Leu531 side chain has rotated away from the binding pocket and is accommodated by a secondary side pocket lined by Lys532 and Ser121 (Figure 1A). There are also minor local structural relaxation changes accompanying the leucine side chain rotation. As the binding site opens and increases in size, inhibitors can make use of the larger binding pocket.

To investigate the stability of these two conformations, PMF calculations were performed for the apoenzyme and for hCOX-1 in complex with two inhibitors, flurbiprofen (Class I) and ibuprofen (Class II) (Figure 1D). In the apo structure, the closed conformation[30,48] of hCOX-1 is ∼5 kcal mol^{-1} more stable than the open one. These results are consistent with the relative occurrence of closed versus open conformations observed over 500 ns of unbiased MD simulations (Figure 1C), and with reported conformations of apo crystal structures.[30,48] Indeed, although collecting accurate statistics from unbiased MD simulations is much less efficient than PMF calculations, we always observed open → closed transitions along trajectories initiated from the higher-energy open state, as expected. No transitions to the open state were observed for trajectories starting from the closed conformation. The PMF calculations, however, reveal striking effects of different classes of inhibitors on this open−closed conformational equilibrium. The tight-binding Class I compound flurbiprofen strongly stabilizes the open state and reduces its free energy to ∼2 kcal mol^{-1} below the closed state. This essentially demonstrates an "induced-fit" type of binding. In complete contrast to this behavior, a Class II inhibitor (ibuprofen) instead destabilizes the open state even beyond its free energy in the apo structure and also increases the closed → open transition barrier (Figure 1D). This observation immediately leads to the notion that tight binding may be equivalent to exclusive open-state binding. To address this idea quantitatively, calculations of free energies of binding to the different states are clearly needed.

Binding Free Energy Calculations. In experimental instant inhibition assays, the affinities of the different classes of ligands are comparable, while in preincubated assays, there is a marked difference between slow, tight-binding Class I inhibitors and other classes of inhibitors. Class I inhibitors bind in the nanomolar range after preincubation, while reversible Class II and Class III inhibitors bind in the micromolar range regardless of assay type. To address the binding energetics of the different enzyme conformations, we selected 16 inhibitors representing the three different classes (Table 1) and conducted binding free energy calculations utilizing the linear interaction energy (LIE) method[9,43,44] as described previously.[9]

The trajectories were monitored and visually inspected to observe conformational changes during the simulations (Table 1). Interestingly, the competitive reversible Class II inhibitor trajectories starting from the open state consistently converge to the closed conformation (Figure 3A). The resulting binding

DOI: 10.1021/acs.biochem.5b01024
Biochemistry 2015, 54, 7283−7291

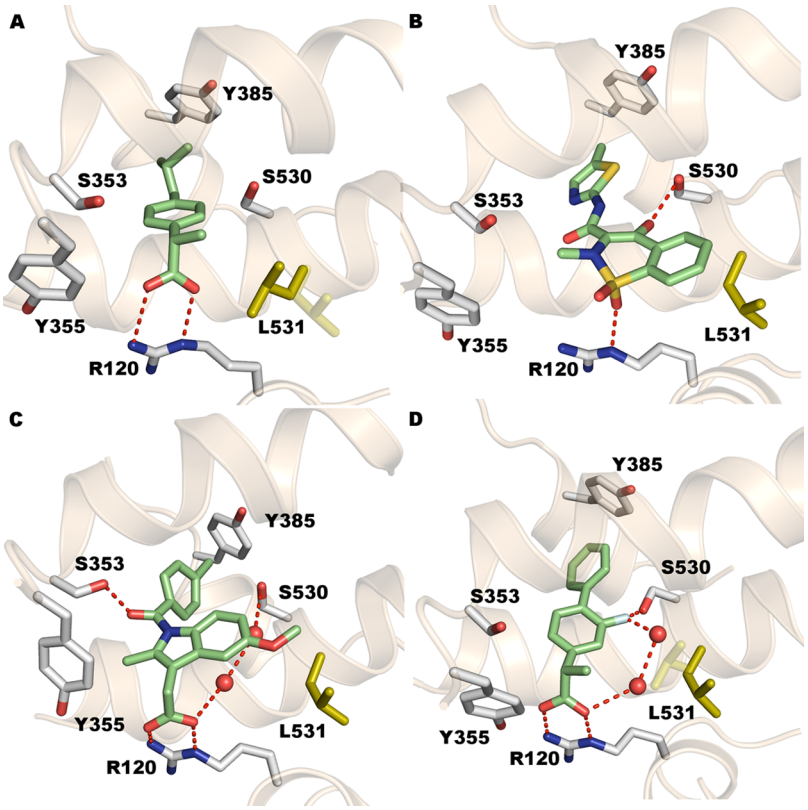

Figure 3. Dominant conformations of Leu531 in hCOX-1 from MD simulations with the following inhibitors: (A) ibuprofen (reversible, Class II), (B) meloxicam (slow, reversible, Class III), (C) indomethacin (slow, tight-binding, Class I), and (D) flurbiprofen (slow, tight-binding, Class I).

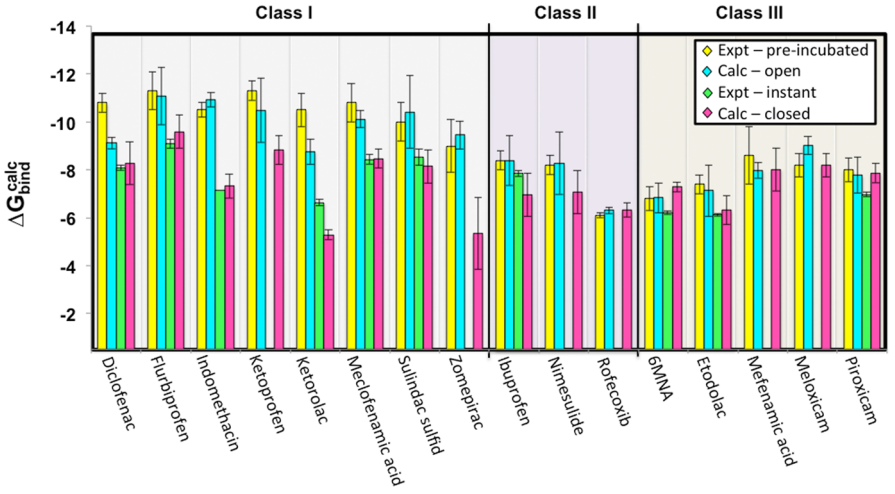

Figure 4. Bar graphs of the experimental and calculated binding free energies (kilocalories per mole). Yellow bars represent the average binding free energies of experimental preincubated assays.[12,13,15−20] The blue and pink bars represent the calculated binding free energies calculated from MD simulations starting from the open and closed[9] conformations, respectively. Green bars represent the experimental binding free energies obtained from instant inhibition assays.[21] Error bars are given as the standard errors of the mean, except for the experimental instant inhibition assay, where it is given as the standard deviation.[21]

free energies are very similar, irrespective of the starting point, reflecting the fact that the intrinsic (apo) free energy difference between the two states persists in the enzyme complexes (Figure 1D). Thus, the calculated binding free energies for the three inhibitors are dominated by the closed conformation, and the predicted binding free energies agree well with reported experimental affinities of both instant inhibition[21] and preincubated assays[4,12,13,15−20] (Table 1 and Figure 4). Similarly, the slow, reversible Class III inhibitors[7,19,27] do not differ significantly between assay types, or in calculated energies from the open and closed conformations. However, this class of ligands is able to make use of the increased space in the open-state binding pocket. Such complexes remain in the open conformation throughout the simulations (Figure 3B), consistent with the crystal structure of Xu and co-workers.[8,29] The root-mean-square deviation (rmsd) between experimental and average MD structures for the only one of our inhibitors cocrystallized in the open conformation, meloxicam, is 1.7 Å,

DOI: 10.1021/acs.biochem.5b01024
Biochemistry 2015, 54, 7283−7291

which is comparable to the corresponding average rmsd of ligands in the closed state reported previously (1.1 Å).[9]

In contrast to those of reversible inhibitors, binding affinities of tight-binding inhibitors differ markedly between the open and closed conformations. Remarkably, the MD/LIE simulations for the open conformation correctly predict all eight tight binders in the high-affinity range, as measured by the preincubated assays (Table 1). Conversely, these inhibitors are predicted to bind significantly weaker to the closed conformation,[9] but with affinities in good agreement with those from the instant inhibition assays.[21] The predicted binding free energies thus correlate well with the differences in experimental affinities between instant inhibition and preincubated assays. From the binding free energy calculations and the trajectories of the MD simulations, it seems clear that high-affinity binding is associated with the open conformation. It would thus be of great interest if this could be unequivocally tested and proven experimentally. Meanwhile, it is noteworthy that the outliers with underestimated affinity (indomethacin, ketorolac, and zomepirac) in our previous work[9] have significantly higher calculated affinities in the open conformation (Table 1). For instance, zomepirac has a calculated binding free energy of −4.7 kcal mol^{-1} in the closed conformation and −9.0 kcal mol^{-1} in the open conformation, where the latter value is in excellent agreement with the value from the preincubated assay. Similarly, the calculated binding free energies of indomethacin in the closed conformation correspond well to instant inhibition assays,[21] while the open conformation calculations are in excellent agreement with average binding free energies from preincubated assays.[12,13,15−20] For these inhibitors, the increased binding affinity is mainly caused by stronger electrostatic interactions with Arg120, as these bulky ligands cannot attain their optimal orientation in the closed conformation because of steric hindrance. In the open state, however, a shallow pocket is formed among Ser530, Leu531, and Arg120, which facilitates optimal salt bridge formation between Arg120 and the carboxylates of tight-binding inhibitors (Figure 3C).

In the case of smaller, more rod-shaped, slow tight-binding inhibitors such as flurbiprofen, the ligand orientation is conserved in the two protein conformations. The main affinity difference instead originates from the different solvation of the binding site. As Leu531 rotates away into the open conformation, the empty site fills with waters, which improves solvation of the electronegative inhibitor substituent interacting with Ser530 (Figure 3D). Two water molecules remain in the cavity throughout the simulations where they form a hydrogen bond network between Arg120 and Ser530, mediated by the carboxylate and electronegative substituent of the ligand. Although the importance of water interactions for carboxylated COX-1 inhibitors has been previously highlighted,[9] these results show that for rod-shaped slow tight-binding inhibitors, such as flurbiprofen, water interactions are crucial for achieving high-affinity binding.

DISCUSSION

Tight-binding inhibition of COX is associated with slow reversibility, high affinities in the nanomolar range, and COX isomer selectivity.[11,14,27] These features have implications in drug design as the lack of COX selectivity is related to ulcer formation after treatment with NSAIDs, whereas selectivity of either isomer could be important in the development of cancer treatments. It is generally accepted that the high affinities of tight-binding inhibitors can be observed only in assays in which the drug is preincubated with the enzyme prior to addition of the substrate. However, the reason for this time dependency is unknown. In instant inhibition assays, in which the substrate and inhibitor are introduced simultaneously to the enzyme, the affinities of the tight-binding inhibitors are in the micromolar range, similar to other classes of COX inhibitors. Numerous binding affinity studies have been carried out to assay structurally diverse inhibitors.[12,13,15−20] Remarkably, there are no obvious structural features distinguishing tight-binding inhibitors from reversible inhibitors. Structurally very different compounds can thus belong to the same kinetic class, while structurally similar inhibitors can produce distinctly different binding and selectivity profiles (Table 1). Although it is known that the formation of salt bridges to the carboxylates is an important feature of tight-binding inhibitors in COX-1, this feature in itself is not sufficient to explain tight binding.

It has been hypothesized that tight-binding inhibition is a result of conformational changes in the protein.[10,14,22,23] However, crystal structures of both apo and holo COX-1 and COX-2 display conserved binding pockets. Although the features regulating tight binding have not been elucidated, the associated high affinities can be probed experimentally. Recently, we examined the binding affinities of a diverse set of 45 NSAIDs in the hCOX-1 enzyme, by means of ligand docking, molecular dynamics, and free energy calculations.[9] The predictions were in excellent agreement with experiment, with a mean unsigned error of 0.9 kcal mol^{-1} for the binding free energies, although we noticed the heterogeneity of the experimental values from different experiments for some compounds in the data set. In particular, three Class I inhibitors (indomethacin, ketorolac, and zomepirac) were consistently underpredicted when compared with the preincubated assays.[12,13,15−17] However, in that work, we considered only the most frequently observed closed conformation of the COX-1 enzyme. Herein, we compared the binding affinities of several Class I−III inhibitors (Table 1), calculated on the basis of two distinct enzyme conformations, with both instant and preincubated inhibition assays. With this strategy, we are able to elucidate the molecular basis for distinguishing between tight-binding and reversible inhibitors.

By using the recently crystallized open conformation of COX-1, the calculated affinities of all eight tight-binding NSAIDs are considerably higher than those found in previous work,[9] where only the closed conformation model was considered. The structural difference between the two enzyme conformations may seem marginal, because it is limited to a conformational change in Leu531, yet the binding affinities increase by up to 4 kcal mol^{-1} for tight-binding inhibitors (as shown both by experiments and by our calculations). Competitive reversible Class II inhibitors do not show this behavior, and their complexes converge toward the closed conformation during MD simulations. This is also in agreement with the results from our PMF calculations, which show that the closed conformation becomes even more favored in the presence of a Class II inhibitor (Figure 1D). On the other hand, the Class I tight-binding inhibitor complexes consistently retain their open conformations during the simulations. In the case of flurbiprofen, a Class I inhibitor, a spontaneous transition to the open state was also observed earlier (Table 1) when the transition was initiated from the closed state,[9] as would indeed be expected from the PMF (Figure 1D). It is further noteworthy how well the binding data from different sources

DOI: 10.1021/acs.biochem.5b01024
Biochemistry 2015, 54, 7283−7291

agree for this inhibitor. That is, both the binding free energy differences from the two types of assays[12,13,15−21] and our calculated PMF, as well as a kinetic analysis of stepwise inhibition,[49] all yield an ∼2 kcal mol^{-1} difference between the two inhibitory states for flurbiprofen. Interestingly, however, the latter work produced a rather slow transition (∼1 s^{-1}) between the states that may indicate that other conformational factors also are at play, such as the documented allostery and cross-talk between the enzyme monomers.[30,50,51]

It is, however, clear that after initial binding of a tight-binding inhibitor to the closed state, the conformational equilibrium of the enzyme would be displaced toward the open conformation in a time-dependent manner, thereby increasing the affinity toward the nanomolar range. Hence, these results rationalize the tight-binding phenomenon of selective COX-1 inhibitors and may facilitate the development of new COX inhibitors with improved selectivity profiles.

AUTHOR INFORMATION

Corresponding Author

*E-mail: aqvist@xray.bmc.uu.se. Phone: +46 18 471 4109.

Funding

Support from the Swedish Research Council (VR-NT 2014-3688 and VR-M 2014-2118), the eSSENCE e-science initiative, and the Swedish National Infrastructure for Computing (SNIC) is gratefully acknowledged.

Notes

The authors declare no competing financial interest.

ABBREVIATIONS

MD, molecular dynamics; LIE, linear interaction energy; COX, cyclooxygenase; NSAID, nonsteroidal anti-inflammatory drug; PMF, potential of mean force; PDB, Protein Data Bank.

REFERENCES

(1) Steinmeyer, J. (2000) Pharmacological basis for the therapy of pain and inflammation with nonsteroidal anti-inflammatory drugs. *Arthritis res. 2*, 379−385.

(2) Winkelmayer, W. C., Waikar, S. S., Mogun, H., and Solomon, D. H. (2008) Nonselective and cyclooxygenase-2-selective NSAIDs and acute kidney injury. *Am. J. Med. 121*, 1092−1098.

(3) Schneider, V., Lévesque, L. E., Zhang, B., Hutchinson, T., and Brophy, J. M. (2006) Association of selective and conventional nonsteroidal antiinflammatory drugs with acute renal failure: a population-based, nested case-control analysis. *Am. J. Epidemiol. 164*, 881−889.

(4) Bresalier, R. S., Sandler, R. S., Quan, H., Bolognese, J. A., Stat, M., Oxenius, B., Horgan, K., Lines, C., Riddell, R., Morton, D., Lanas, A., Konstam, M. A., and Baron, J. A. (2006) Cardiovascular Events Associated with Rofecoxib in a Colorectal Adenoma Chemoprevention Trial. *N. Engl. J. Med. 355*, 221.

(5) Nussmeier, N. A., Whelton, A. A., Brown, M. T., Langford, R. M., Hoeft, A., Parlow, J. L., Boyce, S. W., and Verburg, K. M. (2005) Complications of the COX-2 inhibitors parecoxib and valdecoxib after cardiac surgery. *N. Engl. J. Med. 352*, 1081−1091.

(6) Solomon, S. D., McMurray, J., Pfeffer, M. A., Wittes, J., Fowler, R., Finn, P., Anderson, W. F., Zauber, A., Hawk, E., and Bertagnolli, M. (2005) Cardiovascular risk associated with celecoxib in a clinical trial for colorectal adenoma prevention. *N. Engl. J. Med. 352*, 1071−1080.

(7) Gupta, R. A., and DuBois, R. N. (2001) Colorectal cancer prevention and treatment by inhibition of cyclooxygenase-2. *Nat. Rev. Cancer 1*, 11−21.

(8) Gupta, R. A., Tejada, L. V., Tong, B. J., Das, S. K., Morrow, J. D., Dey, S. K., and DuBois, R. N. (2003) Cyclooxygenase-1 is Overexpressed and Promotes Angiogenic Growth Factor Production in Ovarian Cancer. *Cancer Res. 63*, 906−911.

(9) Shamsudin Khan, Y., Gutiérrez-de-Terán, H., Boukharta, L., and Åqvist, J. (2014) Toward an Optimal Docking and Free Energy Calculation Scheme in Ligand Design with Application to COX-1 Inhibitors. *J. Chem. Inf. Model. 54*, 1488−1499.

(10) Rome, L. H., and Lands, W. E. M. (1975) Structural requirements for time-dependent inhibition of prostaglandin biosynthesis by anti-inflammatory drugs. *Proc. Natl. Acad. Sci. U. S. A. 72*, 4863−4865.

(11) Walker, M. C., Kurumbail, R. G., Kiefer, J. R., Moreland, K. T., Koboldt, C. M., Isakson, P. C., Seibert, K., and Gierse, J. K. (2001) A three-step kinetic mechanism for selective inhibition of cyclooxygenase-2 by diarylheterocyclic inhibitors. *Biochem. J. 357*, 709−718.

(12) Warner, T. D., Giuliano, F., Vojnovic, I., Bukasa, A., Mitchell, J. A., and Vane, J. R. (1999) Nonsteroid drug selectivities for cyclooxygenase-1 rather than cyclo-oxygenase-2 are associated with human gastrointestinal toxicity: A full in vitro analysis. *Proc. Natl. Acad. Sci. U. S. A. 96*, 7563−7568.

(13) Cryer, B., and Feldman, M. (1998) Cyclooxygenase-1 and Cyclooxygenase-2 Selectivity of Widely Used Nonsteroidal Anti-Inflammatory Drugs. *Am. J. Med. 104*, 413−421.

(14) Kulmacz, R. J., and Lands, W. E. (1985) Stoichiometry and kinetics of the interaction of prostaglandin H synthase with anti-inflammatory agents. *J. Biol. Chem. 260*, 12572−12578.

(15) Brideau, C., Kargman, S., Liu, S., Dallob, A. L., Ehrich, E. W., Rodger, I. W., and Chan, C. C. (1996) A human whole blood assay for clinical evaluation of biochemical efficacy of cyclooxygenase inhibitors. *Inflammation Res. 45*, 68−74.

(16) Patrignani, P., Panara, M. R., Greco, A., Fusco, O., Natoli, C., Iacobelli, S., Cipollone, F., Ganci, A., Créminon, C., and Maclouf, J. (1994) Biochemical and pharmacological characterization of the cyclooxygenase activity of human blood prostaglandin endoperoxide synthases. *J. Pharmacol. Exp. Ther. 271*, 1705−1712.

(17) Kato, M., Nishida, S., Kitasato, H., Sakata, N., and Kawai, S. (2001) Cyclooxygenase-1 and cyclooxygenase-2 selectivity of non-steroidal anti-inflammatory drugs: investigation using human peripheral monocytes. *J. Pharm. Pharmacol. 53*, 1679−1685.

(18) Riendeau, D., Charleson, S., Cromlish, W., Mancini, J. A., Wong, E., and Guay, J. (1997) Comparison of the cyclooxygenase-1 inhibitory properties of nonsteroidal anti-inflammatory drugs (NSAIDs) and selective COX-2 inhibitors, using sensitive microsomal and platelet assays. *Can. J. Physiol. Pharmacol. 75*, 1088−1095.

(19) Glaser, K., Sung, M.-L., O'Neill, K., Belfast, M., Hartman, D., Carlson, R., Kreft, A., Kubrak, D., Hsiao, C.-L., and Weichman, B. (1995) Etodolac selectively inhibits human prostaglandin G/H synthase 2 (PGHS-2) versus human PGHS-1. *Eur. J. Pharmacol. 281*, 107−111.

(20) O'Neill, G. P., Mancini, J. A., Kargman, S., Yergey, J., Kwan, M. Y., Falgueyret, J. P., Abramovitz, M., Kennedy, B. P., Ouellet, M., and Cromlish, W. (1993) Overexpression of human prostaglandin G/H synthase-1 and −2 by recombinant vaccinia virus: inhibition by nonsteroidal anti-inflammatory drugs and biosynthesis of 15-hydroxyeicosatetraenoic acid. *Mol. Pharmacol. 45*, 245−254.

(21) Laneuville, O., Breuer, D. K., Dewitt, D. L., Hla, T., Funk, C. D., and Smith, W. L. (1994) Differential inhibition of human prostaglandin endoperoxide H synthases-1 and-2 by nonsteroidal anti-inflammatory drugs. *J. Pharmacol. Exp. Ther. 271*, 927−934.

(22) Copeland, R. A., Williams, J. M., Giannaras, J., Nurnberg, S., Covington, M., Pinto, D., Pick, S., and Trzaskos, J. M. (1994) Mechanism of selective inhibition of the inducible isoform of prostaglandin. *Proc. Natl. Acad. Sci. U. S. A. 91*, 11202−11206.

(23) Selinsky, B. S., Gupta, K., Sharkey, C. T., and Loll, P. J. (2001) Structural Analysis of NSAID Binding by Prostaglandin H2 Synthase: Time-Dependent and Time-Independent Inhibitors Elicit Identical Enzyme Conformations. *Biochemistry 40*, 5172−5180.

(24) Smith, W. L., and Lands, W. E. M. (1971) Stimulation and Blockade of Prostaglandin Biosynthesis. *J. Biol. Chem. 246*, 6700−6704.

DOI: 10.1021/acs.biochem.5b01024
Biochemistry 2015, 54, 7283−7291

(25) Ouellet, M., and Percival, M. D. (1995) Effect of inhibitor time-dependency on selectivity towards cyclooxygenase isoforms. *Biochem. J. 306*, 247−251.
(26) Morrison, J. F. (1982) The slow-binding and slow, tight-binding inhibition of enzyme-catalysed reactions. *Trends Biochem. Sci. 7*, 102−105.
(27) Gierse, J. K., Koboldt, C. M., Walker, M. C., Seibert, K., and Isakson, P. C. (1999) Kinetic basis for selective inhibition of cyclo-oxygenases. *Biochem. J. 339*, 607−614.
(28) van Ryn, J., Kink-Eiband, M., Kuritsch, I., Feifel, U., Hanft, G., Wallenstein, G., Trummlitz, G., and Pairet, M. (2004) Meloxicam Does Not Affect the Antiplatelet Effect of Aspirin in Healthy Male and Female Volunteers. *J. Clin. Pharmacol. 44*, 777−784.
(29) Xu, S., Hermanson, D. J., Banerjee, S., Ghebreselasie, K., Clayton, G. M., Garavito, R. M., and Marnett, L. J. (2014) Oxicams Bind in a Novel Mode to the Cyclooxygenase Active Site via a Two-water-mediated H-bonding Network. *J. Biol. Chem. 289*, 6799−6808.
(30) Sidhu, R. S., Lee, J. Y., Yuan, C., and Smith, W. L. (2010) Comparison of Cyclooxygenase-1 Crystal Structures: Cross-Talk between Monomers Comprising Cyclooxygenase-1 Homodimers. *Biochemistry 49*, 7069−7079.
(31) Gupta, K., Selinsky, B. S., Kaub, C. J., Katz, A. K., and Loll, P. J. (2004) The 2.0 Å Resolution Crystal Structure of Prostaglandin H 2 Synthase-1: Structural Insights into an Unusual Peroxidase. *J. Mol. Biol. 335*, 503−518.
(32) Marelius, J., Kolmodin, K., Feierberg, I., and Åqvist, J. (1998) Q: a molecular dynamics program for free energy calculations and empirical valence bond simulations in biomolecular systems. *J. Mol. Graphics Modell. 16*, 213−225.
(33) Jorgensen, W. L., Maxwell, D. S., and Tirado-Rives, J. (1996) Development and Testing of the OPLS All-Atom Force Field on Conformational Energetics and Properties of Organic Liquids. *J. Am. Chem. Soc. 118*, 11225−11236.
(34) Jorgensen, W. L., Chandrasekhar, J., Madura, J. D., Impey, R. W., and Klein, M. L. (1983) Comparison of simple potential functions for simulating liquid water. *J. Chem. Phys. 79*, 926−935.
(35) King, G., and Warshel, A. (1989) A surface constrained all-atom solvent model for effective simulations of polar solutions. *J. Chem. Phys. 91*, 3647−3661.
(36) Lee, F. S., and Warshel, A. (1992) A local reaction field method for fast evaluation of long-range electrostatic interactions in molecular simulations. *J. Chem. Phys. 97*, 3100−3107.
(37) Ryckaert, J.-P., Ciccotti, G., and Berendsen, H. J. C. (1977) Numerical integration of the cartesian equations of motion of a system with constraints: molecular dynamics of n-alkanes. *J. Comput. Phys. 23*, 327−341.
(38) Boukharta, L., Gutiérrez-de-Terán, H., and Åqvist, J. (2014) Computational Prediction of Alanine Scanning and Ligand Binding Energetics in G-Protein Coupled Receptors. *PLoS Comput. Biol. 10*, e1003585.
(39) Bjelic, S., Brandsdal, B. O., and Åqvist, J. (2008) Cold Adaptation of Enzyme Reaction Rates. *Biochemistry 47*, 10049−10057.
(40) Brandsdal, B. O., Smalås, A. O., and Åqvist, J. (2001) Electrostatic effects play a central role in cold adaptation of trypsin. *FEBS Lett. 499*, 171−175.
(41) Schrödinger Release 2014-2: MacroModel, version 10.4 (2014) Schrödinger, LLC, New York.
(42) Wallin, G., Härd, T., and Åqvist, J. (2012) Folding-Reaction Coupling in a Self-Cleaving Protein. *J. Chem. Theory Comput. 8*, 3871−3879.
(43) Åqvist, J., Medina, C., and Samuelsson, J.-E. (1994) A new method for predicting binding affinity in computer-aided drug design. *Protein Eng., Des. Sel. 7*, 385−391.
(44) Hansson, T., Marelius, J., and Åqvist, J. (1998) Ligand binding affinity prediction by linear interaction energy methods. *J. Comput.-Aided Mol. Des. 12*, 27−35.
(45) Almlöf, M., Carlsson, J., and Åqvist, J. (2007) Improving the accuracy of the linear interaction energy method for solvation free energies. *J. Chem. Theory Comput. 3*, 2162−2175.
(46) Marelius, J., Hansson, T., and Åqvist, J. (1998) Calculation of ligand binding free energies from molecular dynamics simulations. *Int. J. Quantum Chem. 69*, 77−88.
(47) Cheng, Y.-C., and Prusoff, W. H. (1973) Relationship between the inhibition constant (KI) and the concentration of inhibitor which causes 50% inhibition (I50) of an enzymatic reaction. *Biochem. Pharmacol. 22*, 3099−3108.
(48) Picot, D., Loll, P. J., and Garavito, R. M. (1994) The X-ray crystal structure of the membrane protein prostaglandin H2 synthase-1. *Nature 367*, 243−249.
(49) Callan, O. H., So, O.-Y., and Swinney, D. C. (1996) The Kinetic Factors That Determine the Affinity and Selectivity for Slow Binding Inhibition of Human Prostaglandin H Synthase 1 and 2 by Indomethacin and Flurbiprofen. *J. Biol. Chem. 271*, 3548−3554.
(50) Yuan, C., Rieke, C. J., Rimon, G., Wingerd, B. A., and Smith, W. L. (2006) Partnering between monomers of cyclooxygenase-2 homodimers. *Proc. Natl. Acad. Sci. U. S. A. 103*, 6142−6147.
(51) Yuan, C., Sidhu, R. S., Kuklev, D. V., Kado, Y., Wada, M., Song, I., and Smith, W. L. (2009) Cyclooxygenase Allosterism, Fatty Acid-mediated Cross-talk between Monomers of Cyclooxygenase Homodimers. *J. Biol. Chem. 284*, 10046−10055.

DOI: 10.1021/acs.biochem.5b01024
Biochemistry 2015, 54, 7283−7291